A wave-based numerical approach for fast analysis of the dynamic response of periodic structures with local perturbations

Jean-Mathieu Mencik, Denis Duhamel

A wave-based numerical approach for fast analysis of the dynamic response of periodic structures with local perturbations

J.-M. Mencik [1], **D. Duhamel** [2]

[1] INSA Centre Val de Loire, Université François Rabelais de Tours, LMR EA 2640, Campus de Blois, 3 Rue de la Chocolaterie, CS 23410, 41034 Blois Cedex, France
e-mail: **jean-mathieu.mencik@insa-cvl.fr**

[2] Université Paris-Est, Laboratoire Navier, ENPC/IFSTTAR/CNRS, 6 et 8 Avenue Blaise Pascal, Cité Descartes, Champs-sur-Marne, 77455 Marne La Vallée Cedex 2, France
e-mail: **denis.duhamel@enpc.fr**

Abstract

A wave finite element (WFE) based approach is proposed to analyze the dynamic behavior of finite-length periodic structures which are made up of identical substructures but also contain several substructures whose material and geometric characteristics are slightly perturbed. Within the WFE framework, a model reduction technique is proposed which involves partitioning a whole periodic structure into one central structure surrounded by two unperturbed substructures, and considering perturbed parts which are composed of perturbed substructures surrounded by two unperturbed ones. In doing so, a few wave modes are only required for modeling the central periodic structure, outside the perturbed parts. For forced response computation purpose, a reduced wave-based matrix formulation is established which follows from the consideration of transfer matrices between the right and left sides of the perturbed parts. Numerical experiments are carried out on a periodic 2D structure with two perturbed substructures which can be randomly located. The relevance of the WFE-based approach is clearly established in comparison with the FE method, in terms of accuracy and computational saving. Additional simulations are made to examine the feasibility to improve the robustness of periodic structures to the occurrence of a arbitrary slight perturbation, by artificially adding several “controlled” perturbed substructures.

1 Introduction

The study of the dynamic behavior of finite-length periodic structures with local perturbations is addressed within the present paper. Those structures are made up of identical substructures, which can be of arbitrary shapes and are assembled along a certain straight direction. In addition, they contain several perturbed substructures whose material and geometric characteristics undergo arbitrary slight variations. Assessing the sensitivity of the frequency response functions (FRFs) of periodic structures to the occurrence of those perturbed substructures which can be arbitrarily located — e.g., such as variabilities of the design processes, or defects — relates the motivation of the present study. The challenge concerns the development of a numerical approach which is low time-consuming in comparison with the conventional FE method, while keeping the same level of accuracy. The wave finite element (WFE) is investigated to address this task. Indeed the WFE method has proved to be relevant for modeling purely periodic structures like those involving arbitrary-shaped substructures and large-sized FE models, and will be thus improved in this work with a view to modeling periodic structures with local perturbations.

Originally, the WFE method has been developed to describe the wave propagation along one-dimensional periodic structures [1, 2, 3]. The procedure involves considering the finite element (FE) model of a given substructure, and expressing a transfer matrix relation between its right and left boundaries. The sought transfer matrix is symplectic with eigenvectors and eigenvalues which are referred to as wave modes. The eigenvectors are to be understood as wave shapes which propagate from substructure to substructure along the right and left directions of a periodic structure. On the other hand, the eigenvalues have the meaning of wave parameters which are directly linked to the concepts of wavenumbers and wave speeds.

To date, the WFE method has been mainly applied to homogeneous waveguides [4, 5, 6, 7] and simple periodic structures such as truss beams [8] or beams with periodic supports [9]. The strategy to compute the forced response of finite-length periodic structures, which can be subjected to different kinds of boundary conditions, has been investigated in different ways [10, 11, 12, 13]. Recent works have been conducted focusing on the analysis of truly periodic structures of relative complexity [14, 15]. In [15], a model reduction technique has been proposed which enables fast computation of the forced response of periodic structures composed of substructures of arbitrary shape and modeled with many degrees of freedom (DOFs). In this framework, a periodic structure is partitioned into one central structure which is modeled by means of the WFE method, and two surrounding substructures which are modeled with the FE method. In doing so, a few wave modes are only required for modeling the central structure, which is explained by the fact that the kinematic and mechanical fields admit smooth variations on its boundaries. This WFE-based model reduction technique has been proved to be relevant for computing the forced response of a periodic structure with heterogeneous substructures modeled with more than $30,000$ DOFs. The remarkable feature of the approach is that it can be easily implemented on MATLAB®, and yields small computational times when compared to dedicated FE softwares.

The approach proposed in [15] is considered and improved in the present work with a view to modeling periodic structures with local perturbations. In this framework, it is proposed to partition a whole periodic structure into one central structure surrounded by two unperturbed substructures, and introduce perturbed parts which are composed of perturbed substructures surrounded by two unperturbed ones. In doing so, a few wave modes are only required for modeling the central periodic structure, outside the perturbed parts. For forced response computation purpose, a reduced wave-based matrix formulation is established which follows from the consideration of transfer matrices between the right and left sides of the perturbed parts.

The rest of the paper is organized as follows. The WFE method is briefly presented in Section 2. The strategies used to compute the wave modes and the forced response of periodic structures are recalled. The analysis of periodic structures with perturbed substructures is carried out in Section 3. A derivation of the transfer matrices of the perturbed parts is proposed. Also, the wave-based formulation used to compute the forced response of periodic structures with perturbed substructures is presented. In Section 4, numerical experiments are carried out on a periodic 2D structure with two perturbed substructures. Monte Carlo simulations are performed with a view to assessing the sensitivity of the FRFs to the occurrence of arbitrarily-located perturbations. A robust design strategy is also proposed which consists in artificially adding several “controlled” perturbed substructures for lowering the sensitivity of the FRFs to the occurrence of other uncontrolled perturbations.

2 WFE method

2.1 Wave propagation

The WFE method aims at describing the wave propagation along one-dimensional periodic structures like the one shown in Figure 1. These are composed of identical substructures — which are assumed to be linear, elastic and damped by means of a constant loss factor η — which are assembled along a certain straight direction. Also, the substructures are modeled with the same FE mesh and with the same number of DOFs n on their left and right boundaries.

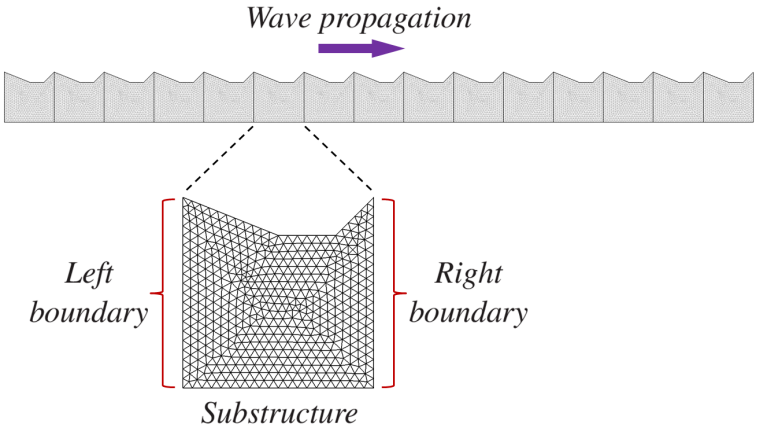

Figure 1: FE mesh of a periodic structure and related substructure.

Denote as $\mathbf{D}$ the dynamic stiffness matrix (DSM) of a given substructure, expressed by $\mathbf{D} = -\omega^2\mathbf{M} + (1+\mathtt{i}\eta)\mathbf{K}$ where $\mathbf{M}$ and $\mathbf{K}$ are the mass and stiffness matrices of the substructure, respectively, and ω is the angular frequency. Also, denote as $\mathbf{D}^*$ the DSM condensed on the left and right boundaries of the substructure, expressed by $\mathbf{D}^* = \mathbf{D}_{\mathtt{BB}} - \mathbf{D}_{\mathtt{BI}}\mathbf{D}_{\mathtt{II}}^{-1}\mathbf{D}_{\mathtt{IB}}$ where subscripts $\mathtt{B}$ and $\mathtt{I}$ refer to the boundary and internal DOFs, respectively.

Within the WFE framework, a transfer matrix relation is considered which links the kinematic/mechanical quantities between the substructures, as follows [3]:

$$\begin{bmatrix} \mathbf{q}_{\mathtt{L}}^{(k+1)} \\ -\mathbf{F}_{\mathtt{L}}^{(k+1)} \end{bmatrix} = \mathbf{S} \begin{bmatrix} \mathbf{q}_{\mathtt{L}}^{(k)} \\ -\mathbf{F}_{\mathtt{L}}^{(k)} \end{bmatrix} \quad , \quad \begin{bmatrix} \mathbf{q}_{\mathtt{R}}^{(k+1)} \\ \mathbf{F}_{\mathtt{R}}^{(k+1)} \end{bmatrix} = \mathbf{S} \begin{bmatrix} \mathbf{q}_{\mathtt{R}}^{(k)} \\ \mathbf{F}_{\mathtt{R}}^{(k)} \end{bmatrix}, \tag{1}$$

where superscript (k) (resp. $(k+1)$) denotes the coupling interface between two consecutive substructures $k-1$ and k (resp. k and $k+1$). Also, $\mathbf{q}$ and $\mathbf{F}$ are $n \times 1$ vectors of nodal displacements and nodal forces, respectively, while subscripts $\mathtt{L}$ and $\mathtt{R}$ refer to the DOFs on the left and right boundaries of the substructures, respectively. In Eq. (1), $\mathbf{S}$ is a $2n \times 2n$ symplectic matrix [2], given by:

$$\mathbf{S} = \begin{bmatrix} -\mathbf{D}_{\mathtt{LR}}^{*-1}\mathbf{D}_{\mathtt{LL}}^{*} & -\mathbf{D}_{\mathtt{LR}}^{*-1} \\ \mathbf{D}_{\mathtt{RL}}^{*} - \mathbf{D}_{\mathtt{RR}}^{*}\mathbf{D}_{\mathtt{LR}}^{*-1}\mathbf{D}_{\mathtt{LL}}^{*} & -\mathbf{D}_{\mathtt{RR}}^{*}\mathbf{D}_{\mathtt{LR}}^{*-1} \end{bmatrix}. \tag{2}$$

The eigenvalues and eigenvectors of $\mathbf{S}$ are denoted as μ_j and $\boldsymbol{\phi}_j$, respectively, and are referred to as the wave modes of the periodic structure. The eigenvalues are referred to as the wave parameters, expressed as $\mu_j = \mathtt{exp}(-\mathtt{i}\beta_j d)$ where d is the substructure length while β_j relates wavenumbers. Also, the eigenvectors are referred to as the wave shapes, defined on each substructure interface as $\boldsymbol{\phi}_j = [\boldsymbol{\phi}_{\mathtt{q}j}^T \, \boldsymbol{\phi}_{\mathtt{F}j}^T]^T$ where $\boldsymbol{\phi}_{\mathtt{q}j}$ and $\boldsymbol{\phi}_{\mathtt{F}j}$ are $n \times 1$ vectors of displacement and force components, respectively.

From the numerical point of view, the direct computation of the eigensolutions of the matrix $\mathbf{S}$ is prone to numerical issues. The reason lies in the fact that the matrix of eigenvectors is partitioned into displacement and force components whose orders of magnitude can be largely disparate each other, meaning that the matrix of eigenvectors is ill-conditioned. Instead, an alternative eigensystem based on the $\mathbf{S} + \mathbf{S}^{-1}$ transformation [16] can be considered which overcomes this issue. This strategy has proved to be relevant for computing the wave modes of periodic structures composed of arbitrary-shaped substructures (see [15]).

Due to the fact that the matrix $\mathbf{S}$ is symplectic, its eigenvalues come in pairs as $(\mu_j, 1/\mu_j)$. This leads to the consideration of n right-going wave modes $\{(\mu_j, \boldsymbol{\phi}_j)\}_{j=1,\ldots,n}$ for which $|\mu_j| < 1$, and n left-going wave modes $\{(\mu_j^\star, \boldsymbol{\phi}_j^\star)\}_{j=1,\ldots,n}$ for which $\mu_j^\star = 1/\mu_j$, with $|\mu_j^\star| > 1$. In matrix form, those right-going and left-going wave modes are written as follows:

$$\boldsymbol{\mu} = (\boldsymbol{\mu}^\star)^{-1} = \mathtt{diag}\{\mu_j\}_{j=1,\ldots,n}, \tag{3}$$

$$\boldsymbol{\Phi}_{\mathtt{q}} = \left[\ \phi_{\mathtt{q}1}\, \phi_{\mathtt{q}2} \cdots \phi_{\mathtt{q}n}\ \right] \quad , \quad \boldsymbol{\Phi}_{\mathtt{F}} = \left[\ \phi_{\mathtt{F}1}\, \phi_{\mathtt{F}2} \cdots \phi_{\mathtt{F}n}\ \right], \tag{4}$$

$$\boldsymbol{\Phi}^{\star}_{\mathtt{q}} = \left[\ \phi^{\star}_{\mathtt{q}1}\, \phi^{\star}_{\mathtt{q}2} \cdots \phi^{\star}_{\mathtt{q}n}\ \right] \quad , \quad \boldsymbol{\Phi}^{\star}_{\mathtt{F}} = \left[\ \phi^{\star}_{\mathtt{F}1}\, \phi^{\star}_{\mathtt{F}2} \cdots \phi^{\star}_{\mathtt{F}n}\ \right], \tag{5}$$

where $\boldsymbol{\Phi}_{\mathtt{q}}$, $\boldsymbol{\Phi}_{\mathtt{F}}$, $\boldsymbol{\Phi}^{\star}_{\mathtt{q}}$ and $\boldsymbol{\Phi}^{\star}_{\mathtt{F}}$ are square matrices of size $n \times n$.

2.2 Forced response

The computation of the forced response of a periodic structure, composed of N substructures, involves expanding the vectors of displacements and forces, on a given substructure boundary (k) ($k = 1, \ldots, N+1$), in the basis of wave shapes:

$$\mathbf{q}^{(k)}_{\mathtt{L}} = \mathbf{q}^{(k)}_{\mathtt{R}} = \boldsymbol{\Phi}_{\mathtt{q}}\mathbf{Q}^{(k)} + \boldsymbol{\Phi}^{\star}_{\mathtt{q}}\mathbf{Q}^{\star(k)} \quad , \quad -\mathbf{F}^{(k)}_{\mathtt{L}} = \mathbf{F}^{(k)}_{\mathtt{R}} = \boldsymbol{\Phi}_{\mathtt{F}}\mathbf{Q}^{(k)} + \boldsymbol{\Phi}^{\star}_{\mathtt{F}}\mathbf{Q}^{\star(k)}, \tag{6}$$

where $\mathbf{Q}^{(k)}$ and $\mathbf{Q}^{\star(k)}$ are $n \times 1$ vectors of wave amplitudes. Also, $\mathbf{q}^{(k)}_{\mathtt{L}}$ and $\mathbf{q}^{(k)}_{\mathtt{R}}$ (resp. $\mathbf{F}^{(k)}_{\mathtt{L}}$ and $\mathbf{F}^{(k)}_{\mathtt{R}}$) are to be understood as the vectors of nodal displacements (resp. nodal forces) on the left boundary of substructure k and the right boundary of substructure $k-1$, respectively.

Also, the spatial variation of the wave amplitudes along the periodic structure is governed by [10]:

$$\begin{bmatrix} \mathbf{Q}^{(k+1)} \\ \mathbf{Q}^{\star(k+1)} \end{bmatrix} = \mathbb{T} \begin{bmatrix} \mathbf{Q}^{(k)} \\ \mathbf{Q}^{\star(k)} \end{bmatrix} \qquad k = 1, \ldots, N, \qquad \text{where} \quad \mathbb{T} = \begin{bmatrix} \boldsymbol{\mu} & \mathbf{0} \\ \mathbf{0} & \boldsymbol{\mu}^{-1} \end{bmatrix}. \tag{7}$$

Hence, the vectors of wave amplitudes at the left and right ends of the whole structure can be linked as $\mathbf{Q}^{(N+1)} = \boldsymbol{\mu}^N \mathbf{Q}^{(1)}$ and $\mathbf{Q}^{\star(1)} = \boldsymbol{\mu}^N \mathbf{Q}^{\star(N+1)}$.

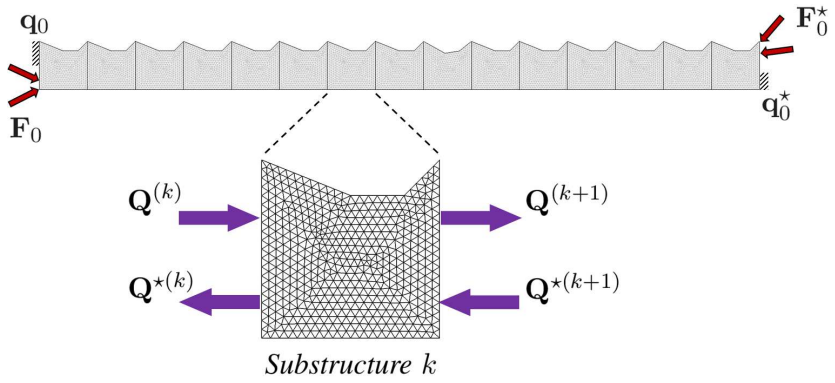

Figure 2: Finite-length periodic structure with prescribed boundary conditions.

The particular case of a periodic structure whose left (resp. right) end is subjected to arbitrary vectors of prescribed displacements $\mathbf{q}_0$ (resp. $\mathbf{q}^{\star}_0$) and forces $\mathbf{F}_0$ (resp. $\mathbf{F}^{\star}_0$) is shown in Figure 2. In this case, the boundary conditions at the left and right ends can be expressed in wave-based form as follows (see [14] for further details):

$$\mathbf{Q}^{(1)} = \mathbb{C}\mathbf{Q}^{\star(1)} + \mathbb{F} \quad , \quad \mathbf{Q}^{\star(N+1)} = \mathbb{C}^{\star}\mathbf{Q}^{(N+1)} + \mathbb{F}^{\star}, \tag{8}$$

where $\mathbb{C}$ and $\mathbb{C}^{\star}$ are $n \times n$ scattering matrices whose components relate the reflection coefficients for the wave modes incident to the boundaries, while $\mathbb{F}$ and $\mathbb{F}^{\star}$ are $n \times 1$ vectors of excitation sources. From Eqs. (7) and (8), a whole matrix equation can be established as follows:

$$\mathcal{A}\mathcal{Q} = \mathcal{F}, \tag{9}$$

where

$$\mathcal{A} = \begin{bmatrix} \mathbf{I}_n & -\mathbb{C}\boldsymbol{\mu}^N \\ -\mathbb{C}^{\star}\boldsymbol{\mu}^N & \mathbf{I}_n \end{bmatrix} \quad , \quad \mathcal{Q} = \begin{bmatrix} \mathbf{Q}^{(1)} \\ \mathbf{Q}^{\star(N+1)} \end{bmatrix} \quad , \quad \mathcal{F} = \begin{bmatrix} \mathbb{F} \\ \mathbb{F}^{\star} \end{bmatrix}. \tag{10}$$

Solving the matrix equation (9) yields the vectors of wave amplitudes $\mathbf{Q}^{(1)}$ and $\mathbf{Q}^{\star(N+1)}$, and by means of Eq. (7) the vectors of wave amplitudes $\mathbf{Q}^{(k)}$ and $\mathbf{Q}^{\star(k)}$ at any substructure boundary (k). Also, the vectors of nodal displacements and nodal forces are simply retrieved from Eq. (6).

3 Modeling of periodic structures with local perturbations

3.1 Framework

To begin, let us consider a periodic structure with N substructures and one perturbed substructure labeled as p. This substructure is perturbed in the sense that its material and geometric properties are slightly different from those of the other substructures. The modeling of the whole perturbed periodic structure is achieved by considering the model reduction technique proposed in [15]. In this framework, the periodic structure is partitioned into one central structure, made up of $N-2$ substructures, and two extra substructures 1 and N, see Figure 3. In doing so, the kinematic and mechanical fields are supposed to admit smooth variations over the interfaces between the central structure and the extra substructures, meaning that they can be described with a few wave modes only. By using the same idea, a perturbed part p can be defined which is composed of the perturbed substructure p and two surrounding unperturbed substructures $p-1$ and $p+1$. The proposed strategy enables the central structure to be modeled with a few wave modes, outside the perturbed part p, which leads to large time saving for forced response computation purpose. The theoretical derivation of the proposed approach is detailed hereafter.

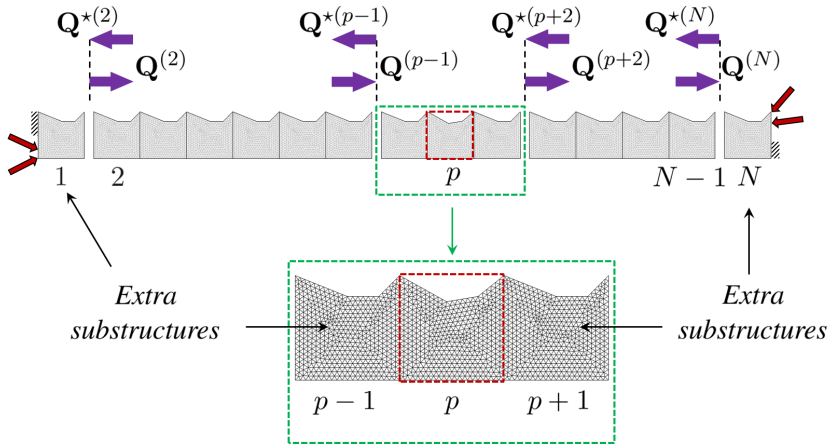

Figure 3: Periodic structure consisting of one central structure surrounded by two unperturbed substructures 1 and N, and containing a perturbed part p made up of a perturbed substructure p surrounded by two unperturbed substructures $p-1$ and $p+1$.

Consider reduced matrices of wave shapes $\widetilde{\mathbf{\Phi}}_{\mathtt{q}} = [\widetilde{\phi}_{\mathtt{q}1} \cdots \widetilde{\phi}_{\mathtt{q}m}]$, $\widetilde{\mathbf{\Phi}}_{\mathtt{F}} = [\widetilde{\phi}_{\mathtt{F}1} \cdots \widetilde{\phi}_{\mathtt{F}m}]$, $\widetilde{\mathbf{\Phi}}^{\star}_{\mathtt{q}} = [\widetilde{\phi}^{\star}_{\mathtt{q}1} \cdots \widetilde{\phi}^{\star}_{\mathtt{q}m}]$ and $\widetilde{\mathbf{\Phi}}^{\star}_{\mathtt{F}} = [\widetilde{\phi}^{\star}_{\mathtt{F}1} \cdots \widetilde{\phi}^{\star}_{\mathtt{F}m}]$ which concern the first m low-order wave modes among the full sets $\{\phi_j\}_{j=1,\ldots,n}$ and $\{\phi^{\star}_j\}_{j=1,\ldots,n}$, i.e., those associated with the values of $|\mu_j|$ and $|\mu^{\star}_j|$ which are the closest to one [1]. Also, denote as $\widetilde{\boldsymbol{\mu}} = \mathtt{diag}\{\widetilde{\mu}_j\}_{j=1,\ldots,m}$ the $m \times m$ diagonal matrix of wave parameters $\widetilde{\mu}_j$ for those low-order wave modes.

As it turns out, a reduced wave expansion can be considered (see Eq. (6)):

$$\widetilde{\mathbf{q}}^{(k)}_{\mathtt{L}} = \widetilde{\mathbf{q}}^{(k)}_{\mathtt{R}} = \widetilde{\mathbf{\Phi}}_{\mathtt{q}}\widetilde{\mathbf{Q}}^{(k)} + \widetilde{\mathbf{\Phi}}^{\star}_{\mathtt{q}}\widetilde{\mathbf{Q}}^{\star(k)} \quad , \quad -\widetilde{\mathbf{F}}^{(k)}_{\mathtt{L}} = \widetilde{\mathbf{F}}^{(k)}_{\mathtt{R}} = \widetilde{\mathbf{\Phi}}_{\mathtt{F}}\widetilde{\mathbf{Q}}^{(k)} + \widetilde{\mathbf{\Phi}}^{\star}_{\mathtt{F}}\widetilde{\mathbf{Q}}^{\star(k)}. \tag{11}$$

Also, the spatial variation of the wave amplitudes, outside the perturbed part, is governed by (see Eq. (7)):

$$\begin{bmatrix} \widetilde{\mathbf{Q}}^{(k+1)} \\ \widetilde{\mathbf{Q}}^{\star(k+1)} \end{bmatrix} = \widetilde{\mathbb{T}} \begin{bmatrix} \widetilde{\mathbf{Q}}^{(k)} \\ \widetilde{\mathbf{Q}}^{\star(k)} \end{bmatrix}, \qquad \text{where} \quad \widetilde{\mathbb{T}} = \begin{bmatrix} \widetilde{\boldsymbol{\mu}} & \mathbf{0} \\ \mathbf{0} & \widetilde{\boldsymbol{\mu}}^{-1} \end{bmatrix}. \tag{12}$$

On the other hand, the boundary conditions at the left and right ends of the central structure can be expressed in wave-based form as follows (see [15] for further details):

$$\widetilde{\mathbf{Q}}^{(2)} = \widetilde{\mathbb{C}}\widetilde{\mathbf{Q}}^{\star(2)} + \widetilde{\mathbb{F}} \quad , \quad \widetilde{\mathbf{Q}}^{\star(N)} = \widetilde{\mathbb{C}}^{\star}\widetilde{\mathbf{Q}}^{(N)} + \widetilde{\mathbb{F}}^{\star}. \tag{13}$$

[1] The selection of those low-order wave modes can be carried out by considering the technique proposed in [17].

Finally, the relation linking the wave amplitudes between the right and left sides of the perturbed part p is expressed by (see Figure 3):

$$\begin{bmatrix} \widetilde{\mathbf{Q}}^{(p+2)} \\ \widetilde{\mathbf{Q}}^{\star(p+2)} \end{bmatrix} = \left(\widetilde{\mathbb{T}}^3 + \Delta_p \widetilde{\mathbb{T}}^3 \right) \begin{bmatrix} \widetilde{\mathbf{Q}}^{(p-1)} \\ \widetilde{\mathbf{Q}}^{\star(p-1)} \end{bmatrix}, \tag{14}$$

where $\widetilde{\mathbb{T}}^3 + \Delta_p \widetilde{\mathbb{T}}^3$ represents the transfer matrix of the perturbed part, where

$$\widetilde{\mathbb{T}}^3 = \begin{bmatrix} \widetilde{\boldsymbol{\mu}}^3 & \mathbf{0} \\ \mathbf{0} & \widetilde{\boldsymbol{\mu}}^{-3} \end{bmatrix}. \tag{15}$$

By considering Eqs. (12), (13) and (14), a wave-based matrix equation can be established to compute the forced response of a periodic structure with one or more perturbed substructures (see next section).

As a preliminary study, the transfer matrix $\widetilde{\mathbb{T}}^3 + \Delta_p \widetilde{\mathbb{T}}^3$ has to be expressed, as follows.
Denote as $\mathbf{D}_p^\star$ the DSM of the perturbed part p which is condensed on its left and right boundaries. Hence, the dynamic equilibrium equation of the perturbed part can be written as

$$\begin{bmatrix} \widetilde{\mathbf{F}}_{\mathtt{L}}^{(p-1)} \\ \widetilde{\mathbf{F}}_{\mathtt{R}}^{(p+2)} \end{bmatrix} = \mathbf{D}_p^* \begin{bmatrix} \widetilde{\mathbf{q}}_{\mathtt{L}}^{(p-1)} \\ \widetilde{\mathbf{q}}_{\mathtt{R}}^{(p+2)} \end{bmatrix}. \tag{16}$$

By considering Eqs. (16) and (11), it can be shown that

$$\left[\mathbf{D}_p^* \widetilde{\boldsymbol{\Psi}}_{\mathtt{q}2} - \widetilde{\boldsymbol{\Psi}}_{\mathtt{F}2} \right] \begin{bmatrix} \widetilde{\mathbf{Q}}^{(p+2)} \\ \widetilde{\mathbf{Q}}^{\star(p+2)} \end{bmatrix} = - \left[\mathbf{D}_p^* \widetilde{\boldsymbol{\Psi}}_{\mathtt{q}1} + \widetilde{\boldsymbol{\Psi}}_{\mathtt{F}1} \right] \begin{bmatrix} \widetilde{\mathbf{Q}}^{(p-1)} \\ \widetilde{\mathbf{Q}}^{\star(p-1)} \end{bmatrix}, \tag{17}$$

where

$$\widetilde{\boldsymbol{\Psi}}_{\mathtt{q}1} = \begin{bmatrix} \widetilde{\boldsymbol{\Phi}}_{\mathtt{q}} & \widetilde{\boldsymbol{\Phi}}_{\mathtt{q}}^\star \\ \mathbf{0} & \mathbf{0} \end{bmatrix} \quad , \quad \widetilde{\boldsymbol{\Psi}}_{\mathtt{q}2} = \begin{bmatrix} \mathbf{0} & \mathbf{0} \\ \widetilde{\boldsymbol{\Phi}}_{\mathtt{q}} & \widetilde{\boldsymbol{\Phi}}_{\mathtt{q}}^\star \end{bmatrix}, \tag{18}$$

$$\widetilde{\boldsymbol{\Psi}}_{\mathtt{F}1} = \begin{bmatrix} \widetilde{\boldsymbol{\Phi}}_{\mathtt{F}} & \widetilde{\boldsymbol{\Phi}}_{\mathtt{F}}^\star \\ \mathbf{0} & \mathbf{0} \end{bmatrix} \quad , \quad \widetilde{\boldsymbol{\Psi}}_{\mathtt{F}2} = \begin{bmatrix} \mathbf{0} & \mathbf{0} \\ \widetilde{\boldsymbol{\Phi}}_{\mathtt{F}} & \widetilde{\boldsymbol{\Phi}}_{\mathtt{F}}^\star \end{bmatrix}. \tag{19}$$

As a result, the transfer matrix $\widetilde{\mathbb{T}}^3 + \Delta_p \widetilde{\mathbb{T}}^3$ is given by

$$\widetilde{\mathbb{T}}^3 + \Delta_p \widetilde{\mathbb{T}}^3 = - \left[\mathbf{D}_p^* \widetilde{\boldsymbol{\Psi}}_{\mathtt{q}2} - \widetilde{\boldsymbol{\Psi}}_{\mathtt{F}2} \right]^+ \left[\mathbf{D}_p^* \widetilde{\boldsymbol{\Psi}}_{\mathtt{q}1} + \widetilde{\boldsymbol{\Psi}}_{\mathtt{F}1} \right], \tag{20}$$

where $[\mathbf{D}_p^* \widetilde{\boldsymbol{\Psi}}_{\mathtt{q}2} - \widetilde{\boldsymbol{\Psi}}_{\mathtt{F}2}]^+$ is the left pseudo-inverse of $[\mathbf{D}_p^* \widetilde{\boldsymbol{\Psi}}_{\mathtt{q}2} - \widetilde{\boldsymbol{\Psi}}_{\mathtt{F}2}]$.

3.2 Forced response

Consider a periodic structure composed of N substructures and containing a certain number P of perturbed parts p_i ($i = 1, \ldots, P$). The concept of perturbed part p_i has been originally introduced to designate a perturbed substructure p_i surrounded by two unperturbed ones. It can be easily extended so as to model a set of two (or more) consecutive perturbed substructures, surrounded by two unperturbed substructures. However, for the sake of clarity, such a case will not be treated here.

By considering Eqs. (12) and (14), a simple relation can be derived which links the vectors of wave amplitudes at any substructure boundary $(k+1)$, inside the central structure and outside the perturbed parts p_i, to those at the left end of the central structure:

$$\begin{bmatrix} \widetilde{\mathbf{Q}}^{(k+1)} \\ \widetilde{\mathbf{Q}}^{\star(k+1)} \end{bmatrix} = \widetilde{\mathbb{T}}^{(k-1)-p_u} \prod_{i=0}^{u-1} \left(\widetilde{\mathbb{T}}^3 + \Delta_{p_{u-i}} \widetilde{\mathbb{T}}^3 \right) \widetilde{\mathbb{T}}^{p_i^u - 3} \begin{bmatrix} \widetilde{\mathbf{Q}}^{(2)} \\ \widetilde{\mathbf{Q}}^{\star(2)} \end{bmatrix}, \tag{21}$$

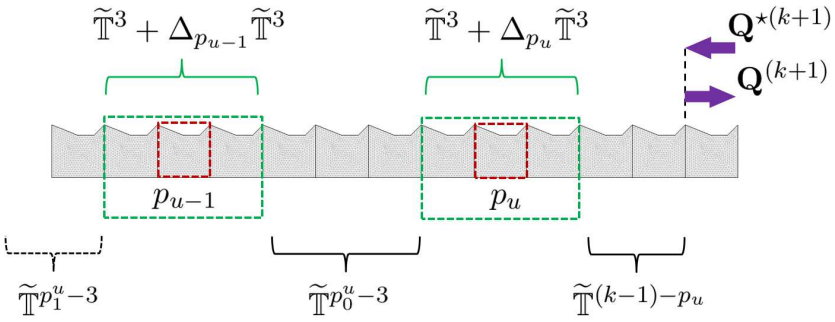

Figure 4: Illustration of the perturbed and unperturbed parts, and related transfer matrices.

where $p_i^u = p_{u-i} - p_{u-i-1}$ for $i \neq u-1$ and $p_{u-1}^u = p_1$, while p_u refers to the perturbed part which is the closest to substructure boundary $(k+1)$. In Eq. (21), $\widetilde{\mathbb{T}}^3 + \Delta_{p_{u-i}}\widetilde{\mathbb{T}}^3$ refers to the transfer matrices of the perturbed parts p_{u-i} $(i = 0, \ldots, u-1)$, while $\widetilde{\mathbb{T}}^{(k-1)-p_u}$ and $\widetilde{\mathbb{T}}^{p_i^u-3}$ refer to the transfer matrices of the unperturbed parts, i.e., between the perturbed parts (see Figure 4).

Also, the vectors of wave amplitudes at the left and right ends of the central structure can be linked as, see Eq. (21):

$$\begin{bmatrix} \widetilde{\mathbf{Q}}^{(N)} \\ \widetilde{\mathbf{Q}}^{\star(N)} \end{bmatrix} = \left(\widetilde{\mathbf{\Lambda}} + \Delta\widetilde{\mathbf{\Lambda}}\right) \begin{bmatrix} \widetilde{\mathbf{Q}}^{(2)} \\ \widetilde{\mathbf{Q}}^{\star(2)} \end{bmatrix}, \tag{22}$$

where $\widetilde{\mathbf{\Lambda}} + \Delta\widetilde{\mathbf{\Lambda}}$ and $\widetilde{\mathbf{\Lambda}}$ are the transfer matrices of the perturbed and unperturbed central structure, respectively:

$$\widetilde{\mathbf{\Lambda}} + \Delta\widetilde{\mathbf{\Lambda}} = \widetilde{\mathbb{T}}^{(N-2)-p_P} \prod_{i=0}^{P-1} \left(\widetilde{\mathbb{T}}^3 + \Delta_{p_{P-i}}\widetilde{\mathbb{T}}^3\right) \widetilde{\mathbb{T}}^{p_i^P-3}, \tag{23}$$

$$\widetilde{\mathbf{\Lambda}} = \widetilde{\mathbb{T}}^{N-2} = \begin{bmatrix} \widetilde{\boldsymbol{\mu}}^{N-2} & \mathbf{0} \\ \mathbf{0} & \widetilde{\boldsymbol{\mu}}^{-(N-2)} \end{bmatrix}. \tag{24}$$

Also, the wave-based boundary conditions at the left and right ends of the central structure need to be considered, see Eq. (13). From Eqs. (13) and (22), a whole matrix equation can be established:

$$\begin{bmatrix} \widetilde{\mathbf{A}} & \widetilde{\mathbf{B}} \\ -\left(\widetilde{\mathbf{\Lambda}} + \Delta\widetilde{\mathbf{\Lambda}}\right) & \mathbf{I}_{2m} \end{bmatrix} \begin{bmatrix} \widetilde{\mathbf{Q}}^{(2)} \\ \widetilde{\mathbf{Q}}^{\star(2)} \\ \widetilde{\mathbf{Q}}^{(N)} \\ \widetilde{\mathbf{Q}}^{\star(N)} \end{bmatrix} = \begin{bmatrix} \widetilde{\mathbb{F}} \\ \widetilde{\mathbb{F}}^{\star} \\ \mathbf{0} \\ \mathbf{0} \end{bmatrix}, \tag{25}$$

where

$$\widetilde{\mathbf{A}} = \begin{bmatrix} \mathbf{I}_m & -\widetilde{\mathbb{C}} \\ \mathbf{0} & \mathbf{0} \end{bmatrix} \quad , \quad \widetilde{\mathbf{B}} = \begin{bmatrix} \mathbf{0} & \mathbf{0} \\ -\widetilde{\mathbb{C}}^{\star} & \mathbf{I}_m \end{bmatrix}. \tag{26}$$

By condensing the matrix equation (25) w.r.t. the first row block, this gives

$$\left[\widetilde{\mathbf{A}} + \widetilde{\mathbf{B}}\left(\widetilde{\mathbf{\Lambda}} + \Delta\widetilde{\mathbf{\Lambda}}\right)\right] \begin{bmatrix} \widetilde{\mathbf{Q}}^{(2)} \\ \widetilde{\mathbf{Q}}^{\star(2)} \end{bmatrix} = \begin{bmatrix} \widetilde{\mathbb{F}} \\ \widetilde{\mathbb{F}}^{\star} \end{bmatrix}. \tag{27}$$

Solving Eq. (25) enables the vector of wave amplitudes $\widetilde{\mathbf{Q}}^{(2)}$ and $\widetilde{\mathbf{Q}}^{\star(2)}$, at the left end of the central structure, to be expressed, and ultimately the vectors of nodal displacements and nodal forces on any substructure interface along the central structure, outside the perturbed parts.

Notice however that the inversion of the matrix on the left-hand side of Eq. (27) is prone to numerical ill-conditioning, which is particularly due to the occurrence of the matrix terms $\widetilde{\boldsymbol{\mu}}^{N-2}$ and $\widetilde{\boldsymbol{\mu}}^{-(N-2)}$ in $\widetilde{\mathbf{\Lambda}}$,

whose components can be largely disparate each other. To solve this issue, a preconditioner can be used, as follows:

$$\widetilde{\mathbf{\Gamma}} = \begin{bmatrix} \mathbf{I}_m & \mathbf{0} \\ \mathbf{0} & \widetilde{\boldsymbol{\mu}}^{N-2} \end{bmatrix}. \tag{28}$$

Hence, Eq. (27) can be rewritten as

$$\left(\left[\widetilde{\mathbf{A}} + \widetilde{\mathbf{B}} \left(\widetilde{\mathbf{\Lambda}} + \Delta\widetilde{\mathbf{\Lambda}} \right) \right] \widetilde{\mathbf{\Gamma}} \right) \widetilde{\mathbf{\Gamma}}^{-1} \begin{bmatrix} \widetilde{\mathbf{Q}}^{(2)} \\ \widetilde{\mathbf{Q}}^{\star(2)} \end{bmatrix} = \begin{bmatrix} \widetilde{\mathbb{F}} \\ \widetilde{\mathbb{F}}^{\star} \end{bmatrix}, \tag{29}$$

where

$$\widetilde{\mathbf{\Gamma}}^{-1} = \begin{bmatrix} \mathbf{I}_m & \mathbf{0} \\ \mathbf{0} & \widetilde{\boldsymbol{\mu}}^{-(N-2)} \end{bmatrix}. \tag{30}$$

Thus, the vectors of wave amplitudes at the left end of the central structure are obtained as follows:

$$\begin{bmatrix} \widetilde{\mathbf{Q}}^{(2)} \\ \widetilde{\mathbf{Q}}^{\star(2)} \end{bmatrix} = \widetilde{\mathbf{\Gamma}} \left(\left[\widetilde{\mathbf{A}} + \widetilde{\mathbf{B}} \left(\widetilde{\mathbf{\Lambda}} + \Delta\widetilde{\mathbf{\Lambda}} \right) \right] \widetilde{\mathbf{\Gamma}} \right)^{-1} \begin{bmatrix} \widetilde{\mathbb{F}} \\ \widetilde{\mathbb{F}}^{\star} \end{bmatrix}. \tag{31}$$

The vectors of wave amplitudes, at any interface between the unperturbed substructures, follow from Eq. (21), while the vectors of nodal displacements and nodal forces follow from Eq. (11).

In Eq. (31), the size of the matrix $[\widetilde{\mathbf{A}}+\widetilde{\mathbf{B}}(\widetilde{\mathbf{\Lambda}}+\Delta\widetilde{\mathbf{\Lambda}})]\widetilde{\mathbf{\Gamma}}$ is $2m \times 2m$ where m is the number of right/left-going wave modes retained. Past studies have demonstrated the fact that, for a periodic structure with a moderate number of substructures, m can be less than one per mil of the total number of DOFs used to model the whole structure [15], without penalizing the accuracy of the WFE method. This means that the inversion of the matrix $[\widetilde{\mathbf{A}} + \widetilde{\mathbf{B}}(\widetilde{\mathbf{\Lambda}} + \Delta\widetilde{\mathbf{\Lambda}})]\widetilde{\mathbf{\Gamma}}$ can be achieved in a very fast way. As it turns out, Eq. (31) provides a fast and simple way to quantify how much the dynamic behavior of a periodic structure is sensitive to the occurrence of a certain number of perturbed substructures.

4 Numerical experiments

4.1 Periodic structure with two perturbed substructures

The purpose of the present section is to validate, first, the proposed WFE modeling when compared to the conventional FE analysis. Here, the FRF of a periodic 2D structure containing two perturbed substructures is studied. The structure under concern is shown in Figure 5. It is made up of $N = 15$ substructures whose characteristics are: density of $7800kg/m^3$, Young's modulus of $210GPa$, Poisson ratio of 0.3, loss factor of 0.005, length of $0.1m$, height of $0.1m$ and thickness of $0.001m$. The whole structure is clamped on its right end, and it is subjected to a longitudinal point force on the left end. The substructures are meshed in the same way using 2D plane stress linear triangles, with two DOFs per node, leading to 1024 DOFs for each substructure and $n = 42$ DOFs over each left/right boundary. Also, the locations of the perturbed substructures are $p_1 = 10$ and $p_2 = 13$, as shown in Figure 5. In the present case, the perturbed substructures share the same geometrical characteristics, which are however slightly different from the rest of the structure, see Figure 5. Also, their loss factors are different to each other, i.e., 0.005 for substructure $p_1 = 10$ and $\eta = 0.008$ for substructure $p_2 = 13$.

The magnitude of the longitudinal displacement of the perturbed periodic structure, at the excitation point, is assessed at 1000 discrete frequencies which are uniformly spread on a frequency band $[5Hz\,,\,5000Hz]$. Within the WFE framework, the computation of this FRF is achieved by considering Eqs. (31), (21) and (11). Also, only a reduced set of wave modes is considered, i.e., $m = 3$ right/left-going wave modes for modeling the central structure outside the perturbed parts (see Section 3). For comparison purpose, the

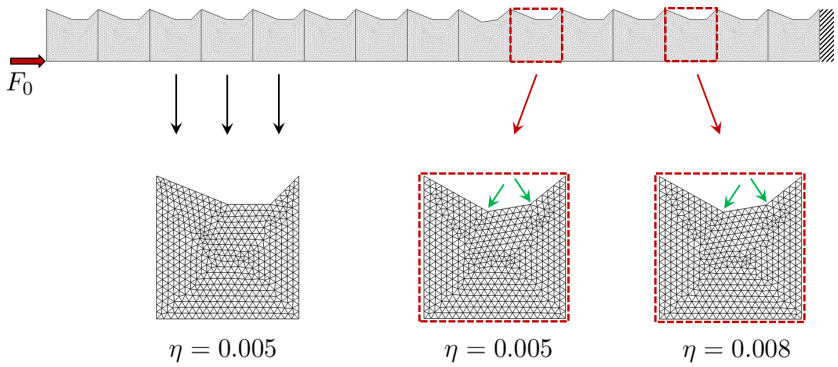

Figure 5: Periodic structure consisting of $N = 15$ substructures and containing two perturbed substructures $p_1 = 10$ and $p_2 = 13$.

FRFs issued from a commercial FE software are also calculated regarding the periodic structure with and without perturbed substructures. The results are shown in Figure 6. As it can be seen, the occurrence of the perturbed substructures significantly impact the FRF of the periodic structure, especially above $4000Hz$. Also, the WFE solution exactly matches the FE-based FRF of the perturbed periodic structure over the whole frequency band. Hence, the accuracy of the proposed modeling is established.

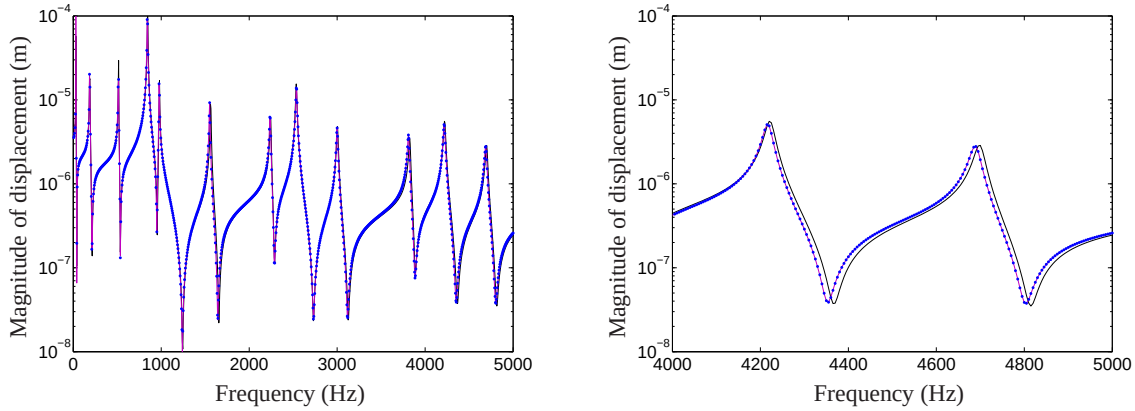

Figure 6: FRF of the periodic structure with two perturbed substructures $p_1 = 10$ and $p_2 = 13$: FE solution (violet solid line); WFE solution (blue dotted line). FE-based FRF of the unperturbed structure (black solid line).

The efficiency of the WFE method lies in the reduction of the computational times. For instance, the proposed approach can be advantageously used to perform Monte Carlo simulations when the locations of the perturbed substructures are randomly chosen along the whole structure. The results are shown in Figure 7. In this case, both perturbed substructures are identical to each other with the same loss factor 0.005. Regarding Figure 7, it should be emphasized that the FRF of the periodic structure becomes more sensitive to the occurrence of the perturbations as the frequency growths. Regarding now the computational times, it takes less than $40s$ with MATLAB® to perform all those simulations with the present approach, against more than $3000s$ with the FE method (and the same processor). Hence, the efficiency of the proposed approach is clearly demonstrated.

4.2 Robust design

The question arises as to whether the sensitivity of periodic structures — i.e., to the occurrence of perturbed substructures which are not controlled — can be lowered by artificially adding several “controlled” perturbed

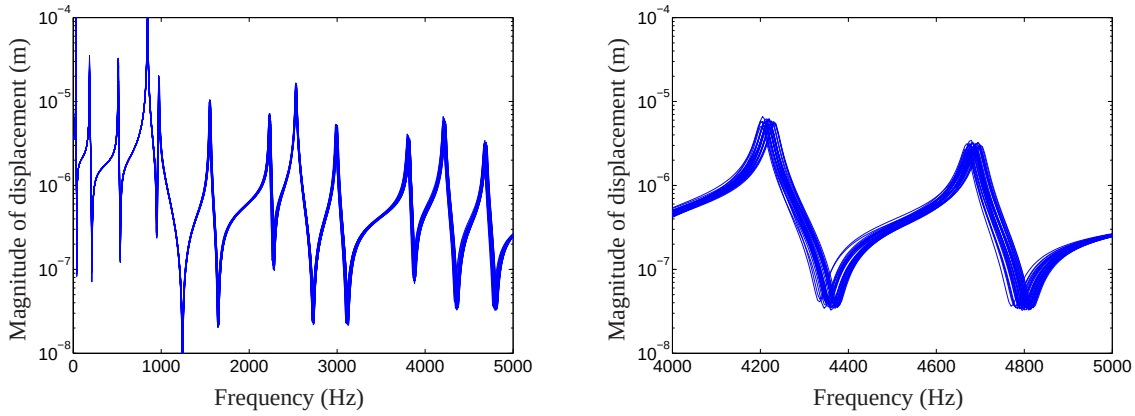

Figure 7: FRF of the periodic structure with two perturbed substructures whose locations arbitrarily vary between $p = 3$ and $p = 13$.

substructures. To address this issue, a periodic structure with $N = 30$ substructures — like those previously described — is considered which contains one "uncontrolled" perturbed substructure whose location along the structure varies randomly. This substructure is slightly perturbed in the sense that its DSM is expressed by $1.05 \times \mathbf{D}^*$, where $\mathbf{D}^*$ relates the DSM of an unperturbed substructure. In addition, two so-called "controlled" perturbed substructures are considered, whose shapes are similar to those of the previously studied perturbed substructures (see Figure 8). These substructures are significantly perturbed in the sense that their DSM is $0.5 \times \mathbf{D}_p^*$, where $\mathbf{D}_p^*$ is the DSM of the perturbed substructures depicted in the previous subsection.

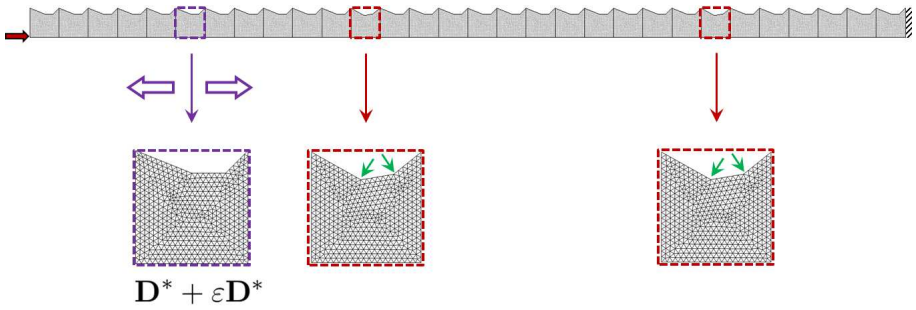

Figure 8: Periodic structure made up of $N = 30$ substructures with two controlled perturbed substructures 12 and 24, and containing one randomly-located uncontrolled perturbed substructure whose DSM is $1.05 \times \mathbf{D}^*$.

Again, MC simulations are performed to assess the FRF of the structure without controlled perturbed substructures over a frequency band $[5Hz\,,\,2500Hz]$ (see Figure 9). For the sake of clarity, the variation/dispersion of the FRF around the resonance peak at $2110Hz$ is also displayed. The purpose behind the present analysis is to assess whether the consideration of the controlled substructures enables the dispersion of the FRF to be reduced, especially around the resonance peak at $2110Hz$. A simple trick is considered here which consists in adding those controlled perturbed substructures at the locations where the periodic structure is the most sensitive to the occurrence of the uncontrolled perturbed substructure. Such an analysis can be simply achieved in a pre-processing step, by calculating the relative error of the displacement response for each possible location of the uncontrolled perturbed substructure. This yields the locations $p_1 = 12$ and $p_2 = 24$ (see Figure 8). Then, the FRF of the periodic structure with controlled perturbed substructures $p_1 = 12$ and $p_2 = 24$, and one randomly-located uncontrolled perturbed substructure [2], is assessed as shown in Figure 10.

As it can be seen, the frequency range with which the FRF is dispersed around the resonance peak decreases

[2]Notice that the locations of the uncontrolled perturbed substructure can match the positions $p_1 = 12$ and $p_2 = 24$ of the controlled perturbed substructures. In this case, the perturbed DSM is $1.05 \times (0.5 \times \mathbf{D}_p^*)$.

from $6.5Hz$ until $5Hz$, i.e., it admits a decrease of 23%. As a second feature, the dispersion of the FRF around the anti-resonance at $2080Hz$ is strongly reduced as shown in Figure 10. Hence, the potentiality of such a robust design is clearly highlighted.

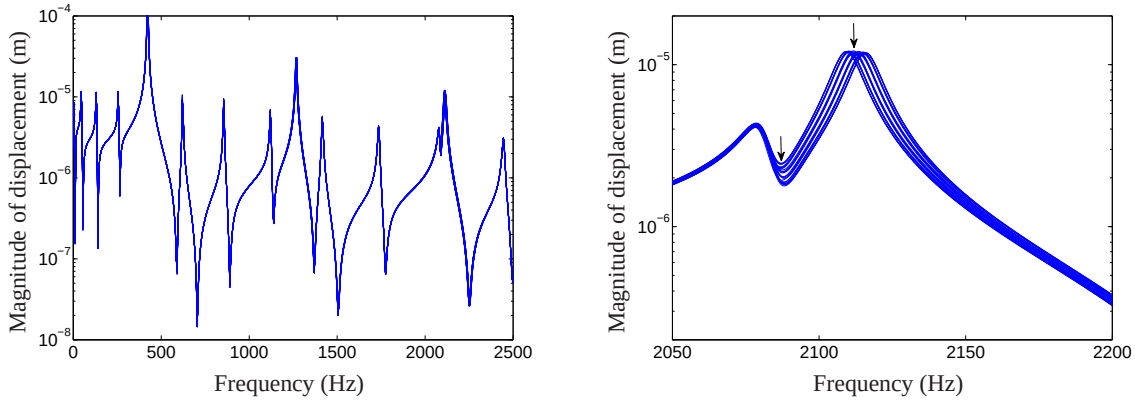

Figure 9: FRF of the periodic structure with one uncontrolled perturbed substructure whose location varies randomly.

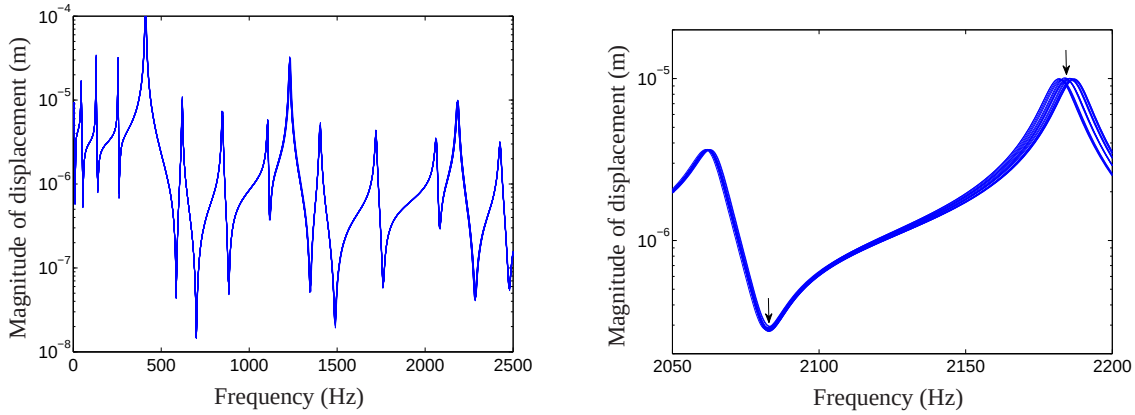

Figure 10: FRF of the periodic structure with two controlled perturbed substructures $p_1 = 12$ and $p_2 = 24$, and with one uncontrolled perturbed substructure whose location varies randomly.

5 Conclusions

The WFE method has been investigated for modeling periodic structures with local perturbations. A model reduction technique has been proposed which enables the dynamic behavior of a whole perturbed periodic structure to be described with a small number of wave modes. A reduced wave-based matrix formulation has been proposed to compute the FRFs of periodic structures in a very fast way. Numerical experiments have been carried out which highlight the relevance of the proposed approach in terms of accuracy and computational saving. In addition, a robust design strategy of periodic structures has been proposed, which consists in artificially adding several controlled perturbations for lowering the sensitivity of the FRFs to the occurrence of uncontrolled perturbations.

References

[1] D. Mead, *A general theory of harmonic wave propagation in linear periodic systems with multiple coupling*, Journal of Sound and Vibration, vol. 27, no. 2, (1973) pp. 235–260.

[2] W. X. Zhong, F. W. Williams, *On the direct solution of wave propagation for repetitive structures*, Journal of Sound and Vibration, vol. 181, no. 3, (1995) pp. 485–501.

[3] J.-M. Mencik, M. N. Ichchou, *Multi-mode propagation and diffusion in structures through finite elements*, European Journal of Mechanics - A/Solids, vol. 24, no. 5, (2005) pp. 877–898.

[4] J.-M. Mencik, M. N. Ichchou, *A substructuring technique for finite element wave propagation in multi-layered systems*, Computer Methods in Applied Mechanics and Engineering, vol. 197, no. 6-8, (2008) pp. 505–523.

[5] B. Mace, D. Duhamel, M. Brennan, L. Hinke, *Finite element prediction of wave motion in structural waveguides*, Journal of the Acoustical Society of America, vol. 117, (2005) p. 2835.

[6] J.-M. Mencik, M. N. Ichchou, *Wave finite elements in guided elastodynamics with internal fluid*, International Journal of Solids and Structures, vol. 44, (2007) pp. 2148–2167.

[7] E. Manconi, B. Mace, R. Gaziera, *Wave finite element analysis of fluid-filled pipes*, Proceedings of NOVEM 2009 “Noise and Vibration: Emerging Methods”, Oxford, UK.

[8] J. Signorelli, A. von Flotow, *Wave propagation, power flow, and resonance in a truss beam*, Journal of Sound and Vibration, vol. 126, no. 1, (1988) pp. 127–144.

[9] L. Gry, C. Gontier, *Dynamic modelling of railway track: a periodic model based on a generalized beam formulation*, Journal of Sound and Vibration, vol. 199, no. 4, (1997) pp. 531–558.

[10] J.-M. Mencik, *On the low- and mid-frequency forced response of elastic systems using wave finite elements with one-dimensional propagation*, Computers and Structures, vol. 88, no. 11-12, (2010) pp. 674–689.

[11] D. Duhamel, B. Mace, M. J. Brennan, *Finite element analysis of the vibrations of waveguides and periodic structures*, Journal of Sound and Vibration, vol. 294, no. 1-2, (2006) pp. 205–220.

[12] Y. Waki, B. Mace, M. Brennan, *Numerical issues concerning the wave and finite element method for free and forced vibrations of waveguides*, Journal of Sound and Vibration, vol. 327, no. 1-2, (2009) pp. 92–108.

[13] J.-M. Mencik, *A wave finite element-based formulation for computing the forced response of structures involving rectangular flat shells*, International Journal for Numerical Methods in Engineering, vol. 95, no. 2, (2013) pp. 91–120.

[14] J.-M. Mencik, *New advances in the forced response computation of periodic structures using the wave finite element (WFE) method*, Computational Mechanics, vol. 54, no. 3, (2014) pp. 789–801.

[15] J.-M. Mencik, D. Duhamel, *A wave-based model reduction technique for the description of the dynamic behavior of periodic structures involving arbitrary-shaped substructures and large-sized finite element models*, Finite Elements in Analysis and Design, vol. 101, (2015) pp. 1–14.

[16] R. Patel, *On computing the eigenvalues of a symplectic pencil*, Linear Algebra and its Applications, vol. 188-189, (1993) pp. 591–611.

[17] J.-M. Mencik, *A model reduction strategy for computing the forced response of elastic waveguides using the wave finite element method*, Computer Methods in Applied Mechanics and Engineering, vol. 229-232, (2012) pp. 68–86.